Electrolyte Management in Porous Battery Components—Static Measurements

Kathleen M. Abbey and Doris L. Britton
Lewis Research Center
Cleveland, Ohio

NASA

ERRATA

NASA Technical Memorandum 83073

ELECTROLYTE MANAGEMENT IN POROUS

BATTERY COMPONENTS - STATIC

MEASUREMENTS

Kathleen M. Abbey and Doris L. Britton
October 1982

Figures 17 and 18: The abscissa scales should be .20, .40, .60, .80 and 0, .20, .40, .60, respectively.

ELECTROLYTE MANAGEMENT IN POROUS BATTERY COMPONENTS - STATIC MEASUREMENTS

Kathleen M. Abbey and Doris L. Britton

National Aeronautics and Space Administration
Lewis Research Center
Cleveland, Ohio 44135

ABSTRACT

The interaction between the porous hydrogen and nickel electrodes and microporous separator with respect to electrolyte management in nickel/hydrogen cells has been investigated. The distribution of electrolyte among the components has been measured and correlated with the pore size distributions, total void volume, and resistance of a variety of electrodes and separators. Calculations are used to show the effects of systematically varying these properties.

INTRODUCTION

Alkaline batteries and fuel cells used in high energy density applications for space are often operated as starved electrolyte systems, i.e., the amount of electrolyte present does not completely saturate the porous components. This contrasts with flooded cells where the electrodes and separators are often immersed in an electrolyte solution. Consequently, the electrolyte distribution in a single plate cell is affected both by the transport phenomena introduced by the presence of a current flowing in the cell and by the competition of the porous components for the available electrolyte. Superimposed on these processes are the factors which affect the electrolyte distribution in a multiplate cell, such as temperature gradients and manufacturing variables. The importance of maintaining an optimum electrolyte volume in starved electrochemical systems has been discussed previously (1). This paper will concentrate on the static effects of pore size engineering among the cell components in order to broaden the volume tolerance of the cell electrolyte content.

The three systems considered are the following: nickel/hydrogen batteries, nickel/cadmium batteries and fuel cells. Table 1 shows the reactions of the repre-

sentative systems. The porous electrodes used are both catalyzed (hydrogen, oxygen) and uncatalyzed (nickel, cadmium). Often the design of matrices and separators for these systems has relied heavily on chemical compatibility considerations of the materials (e.g. corrosion tests in concentrated electrolyte) rather than on properties of the system as a whole (electrodes and separators assembled together in an electrochemical cell). Separators and matrices must be designed for (a) the types of electrodes present in the cell, (b) the respective cell reaction, and (c) the geometrical configuration.

In the first example, the nickel/hydrogen cell consists of both a gas diffusion electrode and a porous nickel hydroxide electrode. Water is both produced and consumed at different electrodes during charging and discharging of the battery. In addition to the reactions listed in Table 1, oxygen is generated at the nickel electrode during the latter half of the charging cycle. Recombination with hydrogen to form water can occur at the catalyzed hydrogen electrode or at a separate recombination electrode. Nickel/cadmium cells consist of two porous electrodes nearly completely filled with electrolyte. Water is consumed at the nickel electrode on discharge and produced during charge so that the battery components will experience a net gain or loss of electrolyte. In alkaline fuel cells, water is produced at the hydrogen electrode and consumed at the oxygen electrode. Because more water is produced than consumed, water is evaporated from the surface of the hydrogen electrode, by regulating the degree of humidification of gas streams. Matrices used in fuel cells always act as gas barriers while separators found in nickel/hydrogen batteries may act as gas barriers depending on the geometrical configuration. Normally, separators used in nickel/cadmium batteries are permeable to gases. These geometrical considerations impose additional requirements on the pore size distributions of the separator and matrix materials.

Proper electrolyte management in batteries and fuel cells requires that the multiplate issues be addressed as well as the single plate concerns. Optimizing porous components so that the optimum current is obtained is important for single plate cells, whereas achieving methods for broadening the tolerance of the cell to changes in the electrolyte content are necessary for the multiplate cell. In the multiplate cell, where groupings of components are assembled together within a com-

mon vessel, the component thicknesses, porosities, and
other variables will assume a statistical distribution
of values. Distribution of parameters such as weight
and thickness will correspond to a distribution of void
volumes from plate to plate within a cell and conse-
quently the electrolyte volume in each component will be
different. Examples of such distributions were given in
an earlier paper (1). This paper will consider the con-
tribution of various factors from an experimental
approach.

Two porous materials which are in contact will ex-
hibit a redistribution of electrolyte through effects of
pore size and wettability. Assuming cylindrical geome-
try, the capillary pressure for a single pore filled
with a wetting (electrolyte) and non-wetting (gas) fluid
is given by

$$p_c = 2\gamma\cos\theta/r \qquad\qquad [1]$$

where θ is the contact angle, γ is the inter-
facial tension between the wetting and non-wetting
fluids in the pore and r is the pore radius (3). Cap-
illary pressure as shown by the equation is a function
of three variables, θ, γ, and r, each of which can
be varied independently. At equilibrium, for two pores
in different materials in contact, the capillary pres-
sures will be equal, $p_1 = p_2$, or

$$2\gamma_1 \cos \theta_1/r_1 = 2\gamma_2 \cos \theta_2/r_2$$

If the pores of the two materials are equally wettable, i.e.
$\theta_1 = \theta_2$ and $\gamma_1 = \gamma_2$, pores of the same radii will be filled
in each. When the contact angles in the materials differ,
$\theta_1 \neq \theta_2$ $\gamma_1 \neq \gamma_2$ pores of different radii will be filled
in each material at equilibrium.

Porous materials do not have pores of uniform size
but instead exhibit a distribution of pore sizes which
leads to an expression for the capillary pressure of

$$p_c = D(r_i) r_i \frac{dp}{dV} \qquad\qquad [2]$$

where $D(r_i)$ is the pore size distribution function and
dV represents the degree of saturation, i.e. the volume
of filled pores. At equilibrium, porous materials in
contact will be saturated to differing degrees as the

3

pore size distributions, wettability, and total porosity will be different. These differing degrees of saturation will affect the cell characteristics (2). The relation between pore structure of components and electrolyte management will now be shown.

EXPERIMENTAL

Properties of both electrodes used in space-weight cells and candidate separator materials for alkaline batteries and fuel cells were studied. The electrodes were obtained from commercial sources as well as some of the separator materials. The composite separators were prepared by placing Zircar (zirconium oxide) cloth onto the screen of a sheet mold and filtering an aqueous solution of fibers and particles through the cloth. Typical properties measured for battery separators using standard techniques (4) are listed in Table 2.

Other measurements were performed as follows:

(a) Scanning electron micrographs were taken on an Amray 1200 B.

(b) Determinations of the pore size distributions were made by mercury intrusion porosimetry (Micromeritics Corp.). Discussions of the technique and data reduction are available (5).

(c) Electrolyte distribution measurements as a function of degree of saturation of the components were made in the Plexiglass cell depicted in Figure 1. The electrodes and separator were oven dried at 90° C overnight and weighed. After the cell was assembled and fastened, it was vacuum impregnated by immersing in solution of 35 percent KOH over which a vacuum was drawn for one hour. The cell was then reassembled and the 35 percent KOH solution added incrementally. After each increment, the cell was undisturbed for one hour in order to allow the electrolyte to equilibrate among the components. The cell was then disassembled and each component weighed in order to determine the electrolyte distribution. This varies from standard techniques (6) which involve withdrawing electrolyte.

(d) Resistance measurements as a function of the total cell electrolyte content were performed in a manner similar to the electrolyte distribution measurements. A General Radio impedance bridge was used.

4

Figures 2 and 3 show pore size distribution curves
for several separators. Polypropylene and Zircar each
have extremely large pore sizes. Celgard has very uni-
form oval shaped pores, 400 x 4000 Å. Because the
holes are not circular, the diameter corresponding to
intrusion only lies in the range of 400-4000 Å, i.e.
diameter of 1300 Å. Beater treated asbestos, fuel
cell grade asbestos with binders and the mixture 20
percent PKT (potassium titanate), 80 percent fuel cell
grade asbestos all show peaks in the pore size distribu-
tion at approximately one micron. The polyethylene In-
terseparator (W. G. Grace) exhibits the broadest distri-
bution of pores. Representative distributions are also
given for electrodes (Figure 4). A greater proportion
of small pores is found in the pore size distribution of
the Air Force nickel electrode (Pickett impregnation
process) than in the distribution of the Comsat elec-
trode (Bell impregnation process). The Air Force hydro-
gen electrode shows a distinctly bimodal distribution
while the pore size distribution of the Comsat electrode
is broader. Also depicted (Figure 5) is the pore size
distribution of a nickel electrode which has been cycled
in a nickel/hydrogen cell. The porosity of the elec-
trode increases with cycling as has been confirmed by
Lim (7). Figures 6 through 10 show the SEM photographs
of some of these materials. Zircar fibers, Figure 6,
are highly oriented to form a knit cloth. Large voids
between individual fibers and holes between the fiber
strands correspond to the largest pores in the size dis-
tribution curves. The individual Zircar fibers are
characterized by deep, rough intrusions or channels.
The polyethylene fibers (Figure 7) are very nodular; the
polypropylene fibers (Figure 8), smooth. The mat com-
posed of fuel cell grade asbestos with 5 percent poly-
vinyl alcohol as a binder (Figure 9) contains a large
range of fiber diameters which allow for very small
pores as predicted from geometrical calculations (8).
The separator composed of 80 percent potassium titanate
fibers and 20 percent zirconium oxide fibers (Figure 10)
is extremely dense. The enlargement of the potassium
titanate fibers reveals that these fibers are extremely
smooth and small. Matrices composed of these fibers
have been studied extensively (9). The SEM for the sep-
arator composed of potassium titanate fibers deposited
on a Zircar cloth (Figure 10) shows that on the under-
side of the Zircar cloth, the PKT fibers adhere to the
Zircar fibers. The difference in size of the two kinds
of fibers is evident in these photos (Figures 10b
and 10c).

5

Electrolyte Distribution Calculations

Based on the pore size distribution, calculated predictions of the static distribution of electrolyte can be made. Assuming that at equilibrium, the capillary pressures between any two components are equal, curves can be constructed based on the mercury intrusion data which show the distribution of electrolyte among the components as a function of the total electrolyte content in the Plexiglass cell, and the percent saturation of the individual components as a function of the total electrolyte content. Figures 11a and 11b give the electrolyte distribution curves calculated using the capillary pressure versus mercury intrusion data for Zircar cloth, an Air Force nickel and an Air Force hydrogen electrode. The Air Force electrodes has been cycled in a nickel/hydrogen cell for only a few formation cycles. These curves predict that on the basis of pore size distribution the Zircar separator acts as a reservoir consistently losing electrolyte to the nickel and hydrogen electrodes. Over a wide range of values of the total cell electrolyte content the percent saturation of the components remains relatively constant while the distribution of electrolyte among the components favors the nickel electrode.

In Figure 12, the calculated electrolyte distribution for a separator containing fuel cell grade asbestos and 5 percent EBL binder is shown. In this case, the model separator was chosen to be approximately 18 mils thick in order to correspond to a separator which had been fabricated in the lab. The separator contains a large fraction of the electrolyte but tends to lose electrolyte to the electrodes when the saturation is less than 100 percent.

The distribution curves for polyethylene Interseparator are given in Figure 13. Because the pore size distribution is very broad the curve showing percent saturation as a function of total cell electrolyte content exhibits several minima and maxima. The electrolyte content of this separator is smaller as the separator is only 5 mils thick. In addition, the lack of wettability of the Teflon in the hydrogen electrode has been taken into account by assuming that approximately three-quarters of the pores are non-wetting. The percent saturation of the hydrogen electrode decreases quite sharply as the cell electrolyte content de-

creases. These types of curves may be constructed for any number of separators or electrodes for which mercury instrusion data are available.

Electrolyte Distribution Measurements

The electrolyte distributions as a function of total cell electrolyte content for a number of combinations of separators and electrodes are shown in Figures 14 and 15. Initially the composite separator (Zircar, FCGA, 5 percent PVA) is filled with an amount of electrolyte equal to that found in the nickel electrode. The separator and nickel electrode lose electrolyte in approximately the same proportion. The hydrogen electrode readily becomes dry at electrolyte contents of the cell less than 100 percent. When the same measurement is repeated with electrodes from a nickel/hydrogen cell of the Air Force configuration which has been cycled for 2600 cycles, the electrodes retain a much larger fraction of the electrolyte than previously. Because the electrodes have been removed from the cell in which they were cycled, this effect cannot be due to compression of the separator resulting from nickel electrode expansion, but must be caused by a change of porosity and pore size in the nickel electrode and a change in wettability of the Teflon in the hydrogen electrode.

The electrolyte distribution for an 18 mil thick separator consisting of fuel cell grade asbestos and 5 percent EBL (Figure 14c) shows that while the separator contains a larger fraction of the cell electrolyte content the nickel electrode strongly competes for the electrolyte. The percent saturation of the nickel electrode remains a higher than that for the separator over the range of cell electrolyte contents measured. The observed curves correlate well for electrolyte contents greater than 50 percent with the curves calculated from pore size considerations shown in Figure 12. In Figure 15a the electrolyte distribution for a Zircar separator and a cycled hydrogen electrode are shown. In this case the separator competes very effectively for the available electrolyte and the nickel electrode shows more of a drying tendency. The electrolyte distribution curves for a cycled nickel electrode and Interseparator (15b) follow very closely the curves predicted on the basis of the pore size distribution.

7

The curves shown in Figure 15c were measured for potassium titanate and zirconium oxide particles deposited onto a Zircar cloth. The electrolyte retention of this separator is high, similar to Zircar cloth when used alone. Figure 16 gives the electrolyte distribution curve for a model composite separator consisting of Zircar cloth, fuel cell grade asbestos with a binder, and Zircar cloth. This curve shows that the Zircar loses electrolyte to the asbestos portion of the separator and the nickel electrode.

Resistance Measurements

The resistances as a function of cell electrolyte content for the configurations of uncycled nickel electrode, separator, and cycled hydrogen electrode are given if Figures 17 and 18. In the first example, Figure 17, the separators used consisted of Zircar cloth, a fuel cell grade asbestos separator with 5 percent EBL binder prepared in the lab and a model composite separator composed of Zircar cloth, fuel cell grade asbestos with 5 percent EBL and Zircar cloth. The resistances of the model separator and the Zircar cloth are much less sensitive to the total electrolyte content than the asbestos separator.

In the second example (Figure 18), the variation of cell resistances with electrolyte content are compared for a separator consisting of fuel cell grade asbestos with binder and for a composite separator consisting of the fuel cell grade asbestos with binder deposited on Zircar cloth. The resistance of the composite separator is again much less sensitive to the electrolyte content than the asbestos.

DISCUSSION

Generally the distribution of electrolyte among the components in the cell and the percent saturation of individual components as a function of total cell electrolyte content correlates well with the pore size distribution with the exception of Zircar cloth where the zirconium oxide fibers are ridged. The degree of hydrogen bonding on the surface of the metal oxide fibers in a concentrated electrolyte such as potassium hydroxide may be expected to be high. In addition, the surface

roughness (10) factor for the deeply ridged fibers will also be large. Both effects result in a smaller contact angle, and hence would be expected to increase the pressures which are required to force a wetting fluid from the pores.

Because the nickel electrode expands during cycling, it is essential to have a separator which functions as a reservoir. However, the resistance of the separator must also be relatively insensitive to the electrolyte content because the amounts of electrolyte will vary in the components of a multiplate cell. In both these respects, the model composite separator consisting of Zircar cloth, asbestos with a binder and Zircar cloth and the composite separator prepared by depositing fuel cell grade asbestos with a binder on Zircar cloth appear to be superior. In addition to the pore size engineering/wettability affects, which include consideration of the thickness of the porous components within the cell, the resistance as a function of compression should be determined in order to predict the geometry of the optimum separator. In addition the dynamic aspects of electrolyte redistribution should be considered.

For the dynamic aspects of electrolyte management in alkaline, starved-electrolyte systems, the following couples should be examined independently:

(a) Fuel Cells - In fuel cells, the gaseous reactants are forced into the cell by pumping. The system operates continuously and does not recharge so that the electrode reactions always proceed in the same direction. After a short start-up interval, the system is operating in a steady state configuration. This implies that the potassium flux,

$$\nabla \cdot J_{K^+} = 0 \qquad\qquad [3]$$

and that

$$\nabla \cdot J_{OH^-} = \text{rate of production or consumption of hydroxide ion.}$$

9

The overall current, $I = (J_+ - J_-)nF$ is then only dependent on the hydroxide ion flux. Assuming that the electrode can be described as a finite slab of cylindrical pores, the hydroxide ion flux may be expressed in cylindrical coordinates as,

$$J = -D_{OH^-}\left[\frac{1}{r}\frac{\partial}{\partial r}(rC_{OH^-}) + \frac{\partial C}{\partial z}_{OH^-}\right] + vC_{OH^-}$$

$$+ D_{OH^-}\left[\frac{1}{r}\frac{\partial}{\partial r}(r\psi) + \frac{\partial \psi}{\partial r}\right] \quad [4]$$

where r is the pore radius, z is the distance along a cylindrical pore, ψ is the potential, v is the volume flux of electrolyte, D is the diffusion coefficient and C is the concentration. Simplifying assumptions such as that of radial symmetry can be introduced and the boundary conditions for the pore made to reflect limiting current conditions. In addition, approximations for the steady state flow of electrolyte, v, which describe the fraction of water allowed to travel to the oxygen electrode and the amount evaporated off the surface of the hydrogen electrode, can be used. By numerical solution of the equations derived and satisfying the boundary conditions for hydrogen electrode, oxygen electrode and fuel cell matrix, the current as a function of pore radius may be calculated. When integrated over the pore size distributions of the components, the total current may be computed. Consequently, optimum pore size distributions from kinetic considerations may be determined. Because the systems are starved electrolyte systems, the amount of electrolyte in each electrode affects the thickness of the film in the pore through which gas must diffuse. The amount of electrolyte present is related to the capillary pressure characteristics. The optimum amount can be engineered by altering the electrode pore size distribution or by varying the Teflon content to change the wetting characteristics.

(b) Nickel/hydrogen batteries - Unlike fuel cells nickel/hydrogen batteries are enclosed in pressure vessels. During charge and discharge, the hydrogen pressure varies from 200 to 600 psig. rather than remaining constant. Because these cells are not operated in a steady state condition, the continuity equation must be used

$$\frac{\partial C}{\partial t}_{OH}^- = \nabla \cdot J_{OH}^- + R_{OH} \qquad [5]$$

where R = Rate of production of OH^- due to the chemical reaction

$$\frac{\partial C}{\partial t}_{OH}^- = J_{K}^+ \qquad [6]$$

when determining the current as a function of pore radius. At each time t, and for distances across the length of the pore of dz and dr, profiles for the concentration and potential must be calculated.

Initially, the static distribution of electrolyte among the cell components is determined by the pore size distribution of their materials. As the cell cycles, the nickel electrode expands and the pore size distribution in the electrode changes. Although the tolerance of the nickel/hydrogen cell to changes in the electrolyte volume is wider than that of a fuel cell, the components do not experience greater morphological changes. Consequently, engineering the pore size distributions to incorporate reservoir properties into the separator is necessary so that the resistance of the separator is less sensitive to electrolyte content.

(c) Nickel/cadmium cells - In nickel/cadmium cells, the separator must have a very wide volume tolerance because a net increase in the amount of water present occurs on charge. The separator must be able to accommodate this change while steadily losing electrolyte to the nickel electrode as cycling occurs. However, the separator may be a very porous material because in the usual geometric configuration, oxygen diffuses through the separator to the cadmium electrode for recombination. Separators which have a high bubble pressure, i.e. a large density of small pores, are not required as in the example of fuel cells.

Electrolyte management has been studied in other fuel cell systems (11).

In conclusion,

(a) Electrolyte management in starved alkaline electrochemical cells is a function of the interactions among all porous components in a cell.

11

(b)   The pore size distributions and wettability of the components determine the capillary pressure characteristics which govern the static distribution of electrolyte among the components.

(c)   Composite separators may be required in order to optimize electrolyte management in nickel/hydrogen and nickel/cadmium batteries.

(d)   The dynamic aspects of electrolyte redistribution should be studied by appropriate modelling in order to distinguish between the requirements for porous components in individual alkaline electrochemical systems.

REFERENCES

(1)   K. M. Abbey and L. H. Thaller, "Pore Size Engineering Applied to Starved Electrochemical Cells and Batteries," National Aeronautics and Space Administration, Washington, D. C., NASA TM 82893 (1982).
(2)   Yu. M. Vol'fkovich, Elektrokhimiya, 14, 546 (1978).
(3)   H. L. Ritter and L. C. Drake, Ind. Eng. Chem., 17, 782 (1945).
(4)   J. E. Cooper and A. Fleischer, "Characteristics of Separators for Alkaline Silver Oxide Zinc Secondary Batteries", A. F. Aero Propulsion Laboratory, Wright-Patterson AFB, OH, (1964).
(5)   S. Lowell, "Introduction of Powder Surface Area," John Wiley, New York (1979).
(6)   S. Verzwyvelt, in "The 1980 Goddard Space Flight Center Battery Workshop," NASA CP-2177, p. 217, National Aeronautics and Space Administration, Washington, D.C. (1981).
(7)   H. Lim in "The 1980 Goddard Space Flight Center Battery Workshop," NASA CP-2177, p. 175, National Aeronautics and Space Administration, Washington, D. C. (1981).
(8)   L. M. Handley, A. P. Meyer, and W. F. Bell, "Development of Advanced Fuel Cell System, Final Report, Phase III, "National Aeronautics and Space Administration, Washington, D. C., NASA CR-134818 (1975).
(9)   Robert E. Post, "Evaluation of Potassium Titanate as a Component of Alkaline Fuel Cell Matrices," National Aeronautics and Space Administration, Washington, D. C., NASA TND-8341 (1976).
(10)   Arthur W. Adamson, "Physical Chemistry of Surfaces," John Wiley, New York (1976).
(11)   H. C. Maru, D. Patel, and L. Paetsch, "Abstracts of Electrochemical Society Meeting," 128, 710 (1981).

Nickel/Hydrogen

$$1/2 \ H_2 + OH^- \longrightarrow H_2O + e^-$$

$$NiOOH + H_2O + e^- \longrightarrow Ni(OH)_2 + OH^-$$

$$\overline{NiOOH + 1/2 \ H_2 \longrightarrow Ni(OH)_2}$$
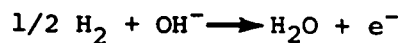
Comment: No net production or consumption of water
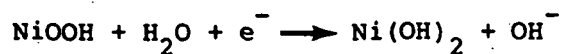
Nickel/Cadmium

$$2 \ NiOOH + 2 \ H_2O + 2e^- \longrightarrow 2 \ Ni(OH)_2 + 2 \ OH^-$$

$$Cd + 2 \ OH^- \longrightarrow Cd(OH)_2 + 2e^-$$

$$\overline{2 \ NiOOH + 2 \ H_2O + Cd \longrightarrow 2 \ Ni(OH)_2 + Cd(OH)_2}$$
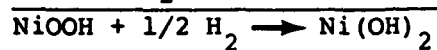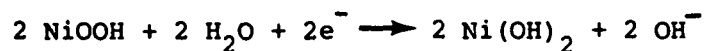
Comment: Water consumed at the nickel elctrode on discharge
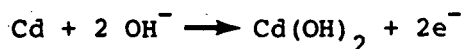
Alkaline Fuel Cells

$$H_2 + 2 \ OH^- \longrightarrow 2 \ H_2O + 2e^-$$

$$2e^- + 1/2O_2 + H_2O \longrightarrow 2 \ OH^-$$

$$\overline{H_2 + 1/2 \ O_2 \longrightarrow H_2O}$$
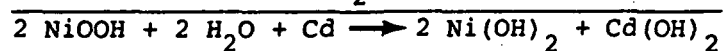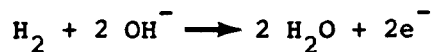
Comment: Water produced at the hydrogen electrode and consumed at the oxygen electrode
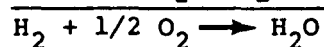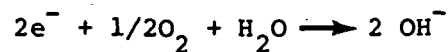
TABLE 2. - SEPARATOR PROPERTIES

Membrane/separator	Volume resistivity (†) Ωcm⁻¹		Percent porosity (†)		Percent porosity (*)	Percent electrolyte retention (†)		Percent change of thickness on wetting	
	35% KOH	45% KOH	35% KOH	45% KOH		35% KOH	45% KOH	35% KOH	45% KOH
FCGA, 5% EBL	9.65	9.14	75.9	72.7	---	152	162	14	27
FCGA, 5% PVA	7.7	4.95	79.1	74.2	---	175	177	---	---
20% PKT, 80% FCGA, 5% EBL	8.08	8.32	71.9	75.4	69.6	138	135	3	12
W.R. Grace Interseparator (Polyethylene)	13.18	1.43	19.1	20.5	76.2	48	57	20	19
Polypropylene	3.8	4.3	24	31	76.8	---	---	18	14
Beater treated asbestos	7.19	3.0	70.6	----	66.2	96	---	----	---
Zircar	4.73	3.33	24.3	19.2	82.6	---	---	.9	4
Celgard (3501)	36	----	48	50	56.2	103	110	----	---

*Determined from mercury instrusion porosimetry.
†Reference 4

14
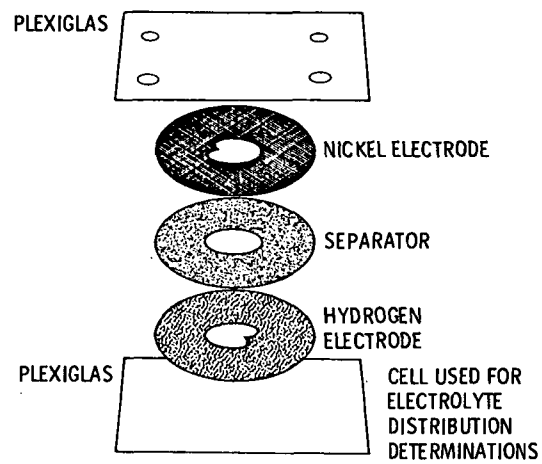
Figure 1. - Cell used for electrolyte distribution determinations.
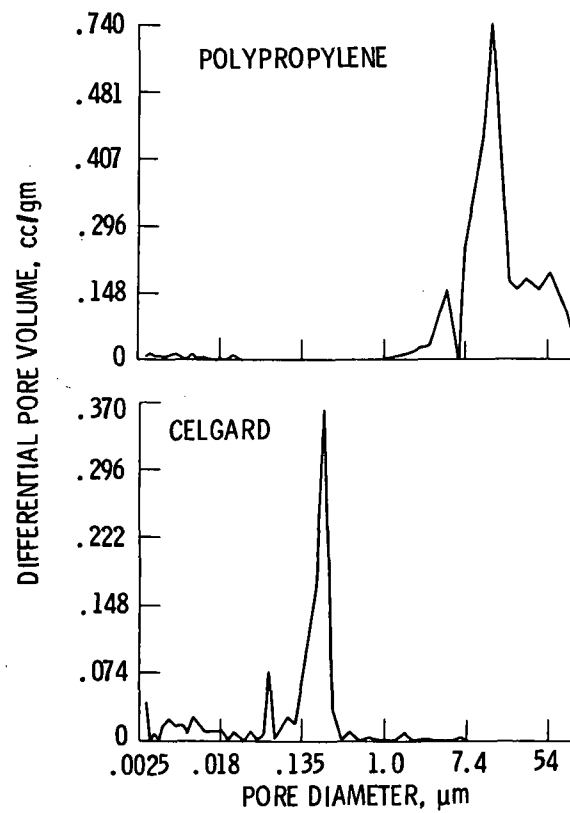
Figure 2. - Pore size distribution curves of separators.
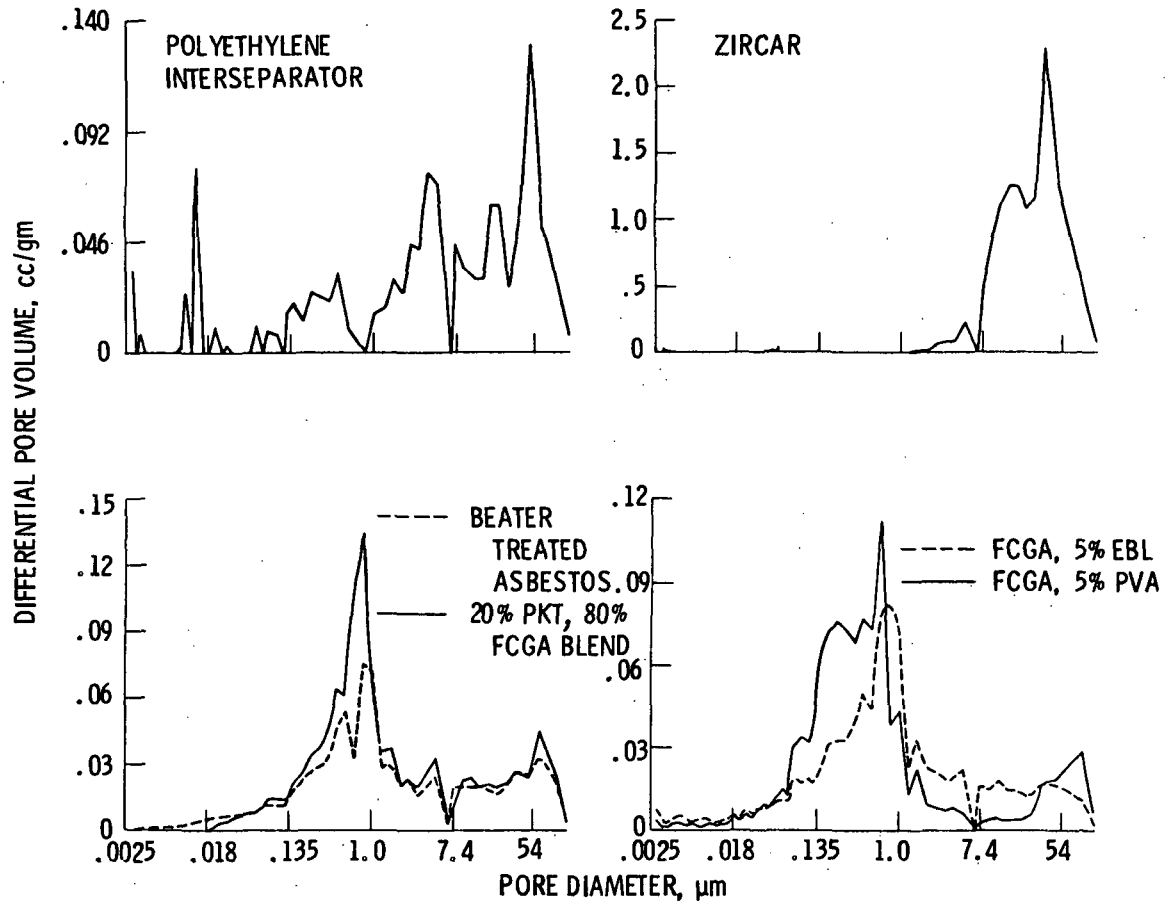
Figure 3. - Pore size distribution curves of separators.

—————— AIR FORCE
— — — — COMSAT

HYDROGEN ELECTRODE

NICKEL ELECTRODE

— — — — AIR FORCE
—————— COMSAT

DIFFERENTIAL PORE VOLUME, cc/gm

PORE DIAMETER, μm
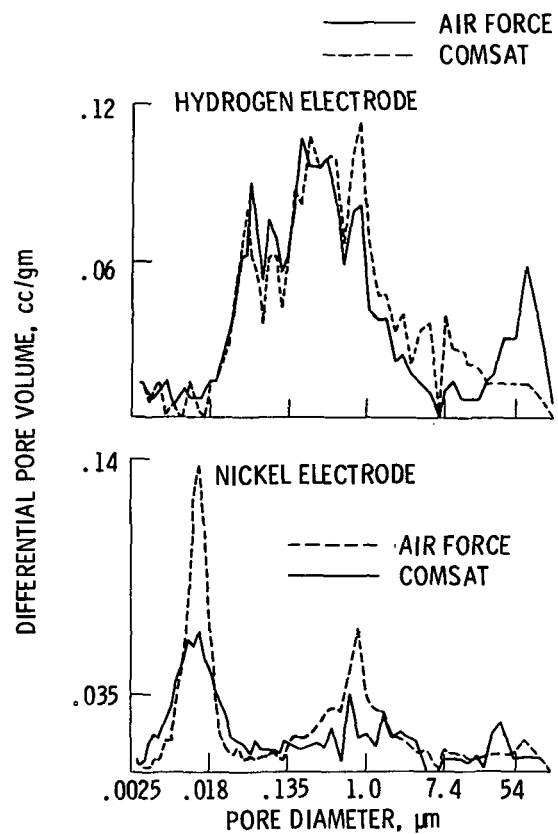
Figure 4. - Pore size distribution curves
of electrodes.

NICKEL ELECTRODE

AIR FORCE
—————— 6 CYCLES
— — — — 260 CYCLES

DIFFERENTIAL PORE VOLUME,
cc/gm

PORE DIAMETER, μm
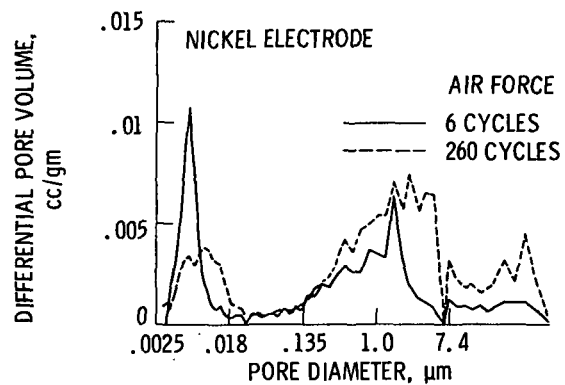
Figure 5. - Cycled electrode pore size
distribution curves.
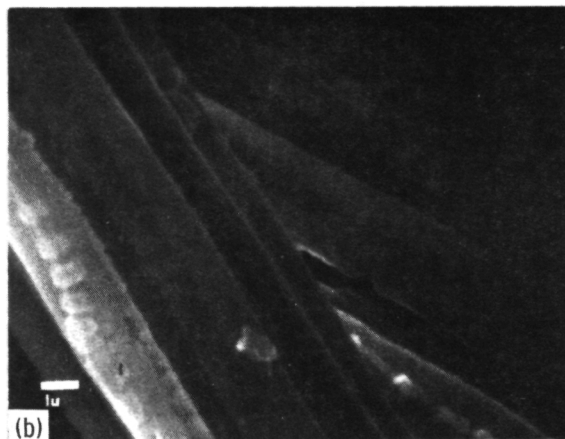
(a) CLOTH.

(b) ENLARGEMENT OF ZIRCAR FIBER.

Figure 6. – SEM of zirconium oxide separator.
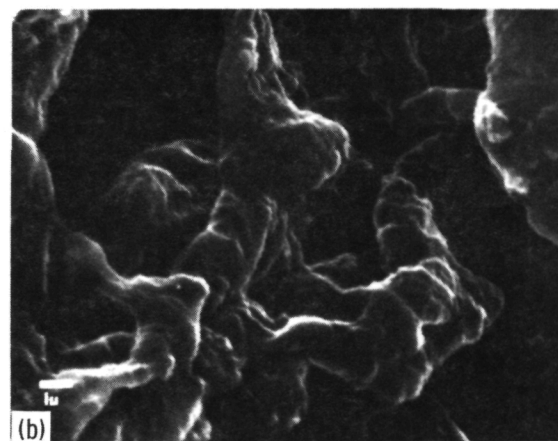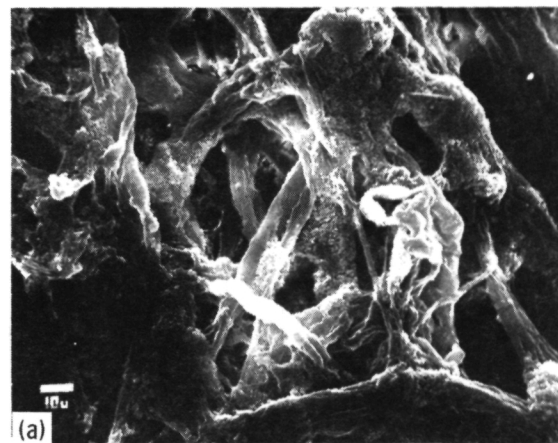
(a) SECTION.

(b) ENLARGEMENT OF SINGLE FIBER.

Figure 7. – SEM of polyethylene Interseparator.
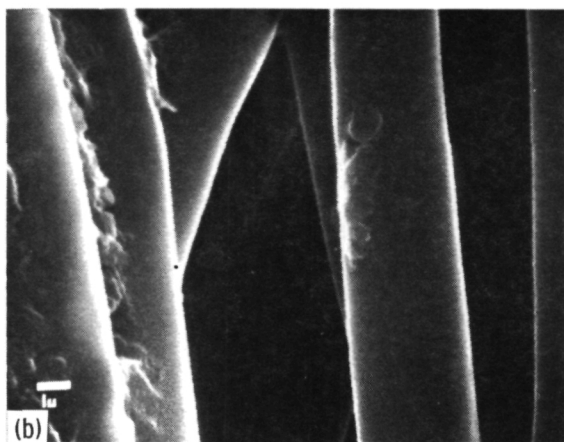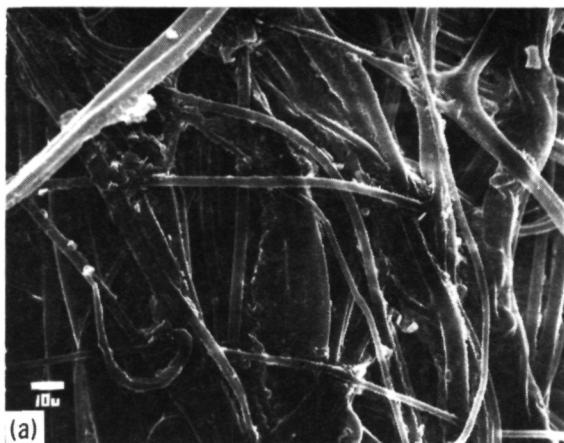
(a) SECTION.

(b) ENLARGEMENT OF SINGLE FIBER.

Figure 8. - SEM of Polypropylene (wettable).
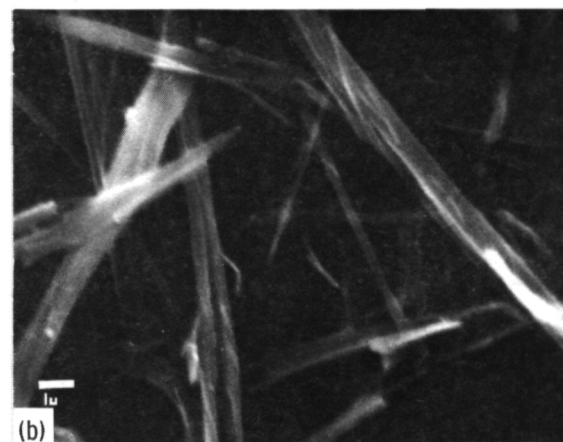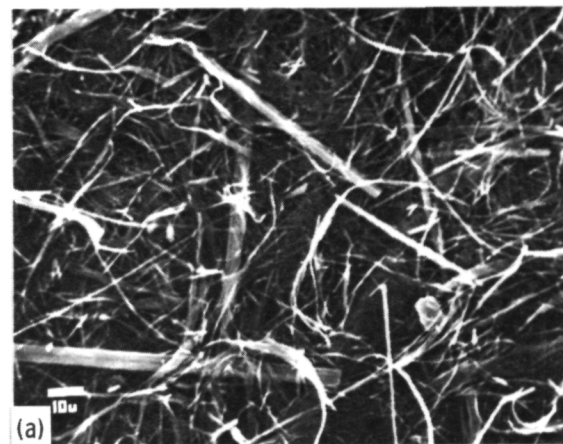
(a) SECTION.

(b) ENLARGEMENT WHICH SHOWS INDIVIDUAL FIBERS.

Figure 9. - SEM of fuel cell grade asbestos with 5% polyvinyl alcohol binder.
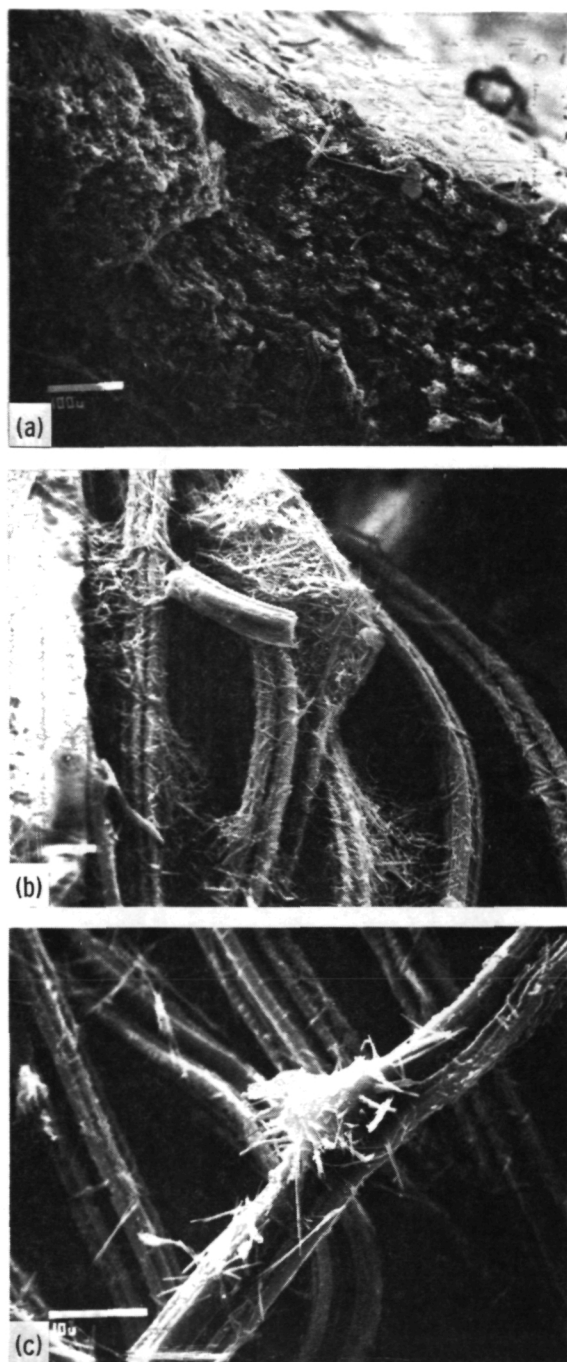
(a) SEPARATOR CONSISTING OF 80% PKT, 20% ZrO_2 FIBERS.

(b) SEPARATOR CONSISTING OF PKT FIBERS ON ZIRCAR CLOTH.

(c) ENLARGEMENT OF (b).

Figure 10. - SEM of potassium titanate separator.
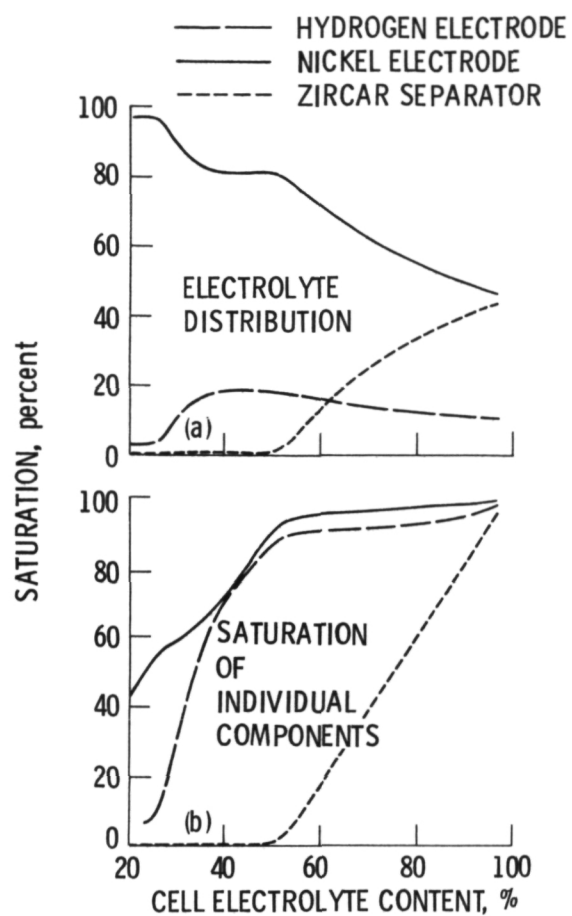
(a) Electrolyte distribution among cell components.

(b) Percent saturation of individual components.

Figure 11. - Zircar.
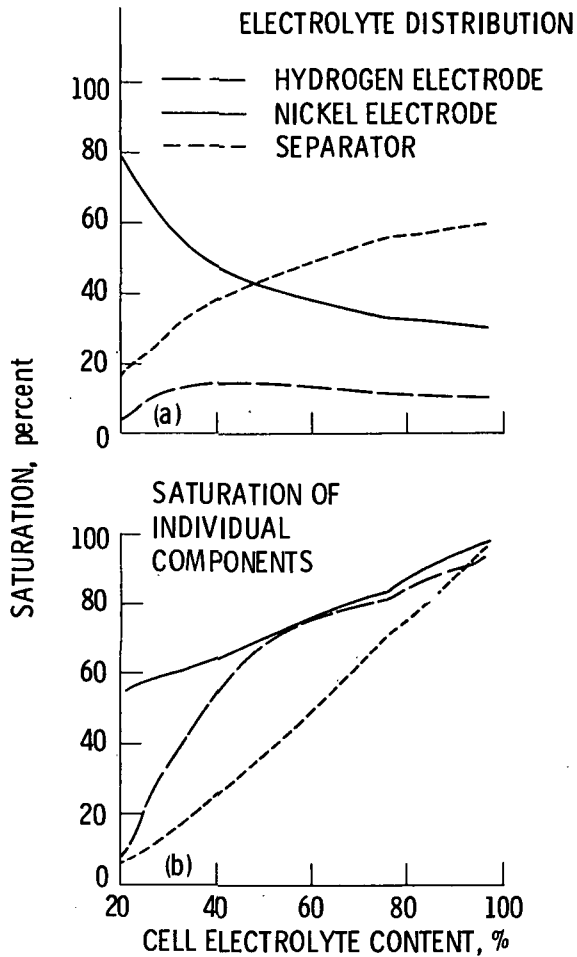
(a) Electrolyte distribution among cell components.

(b) Percent saturation of individual components.

Figure 12. - FCGA with binder.
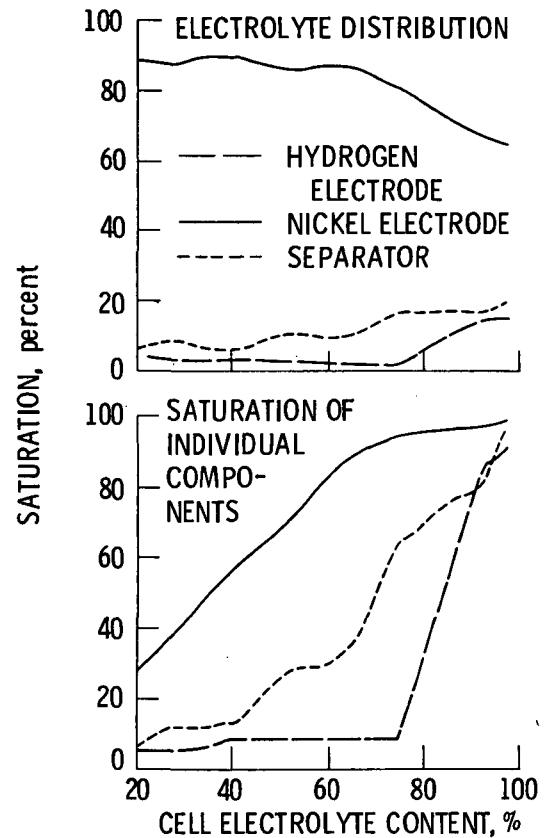
(a) Electrolyte distribution among cell components.

(b) Percent saturation of individual components.

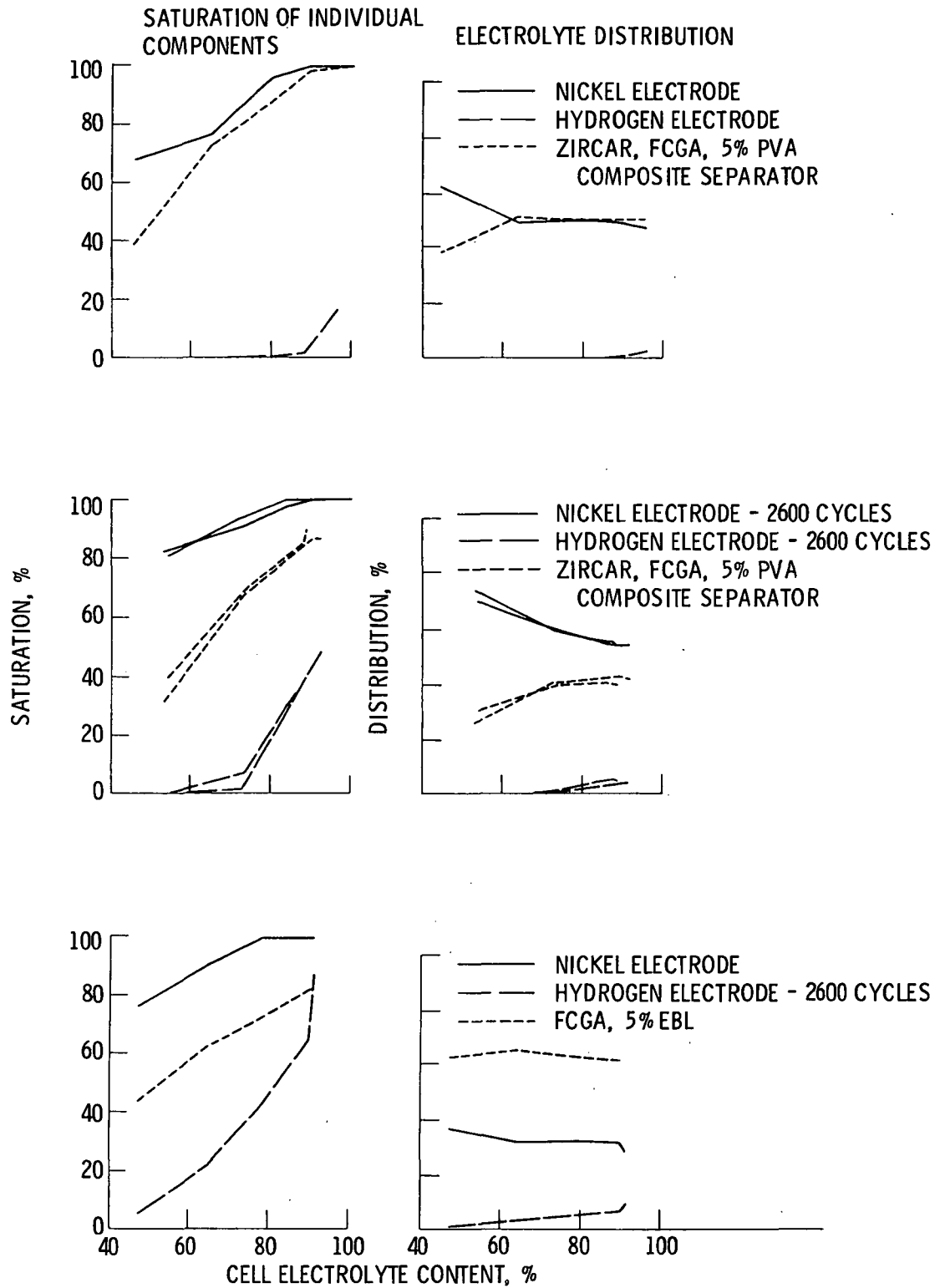Figure 13. - Polyethylene Interseparator.

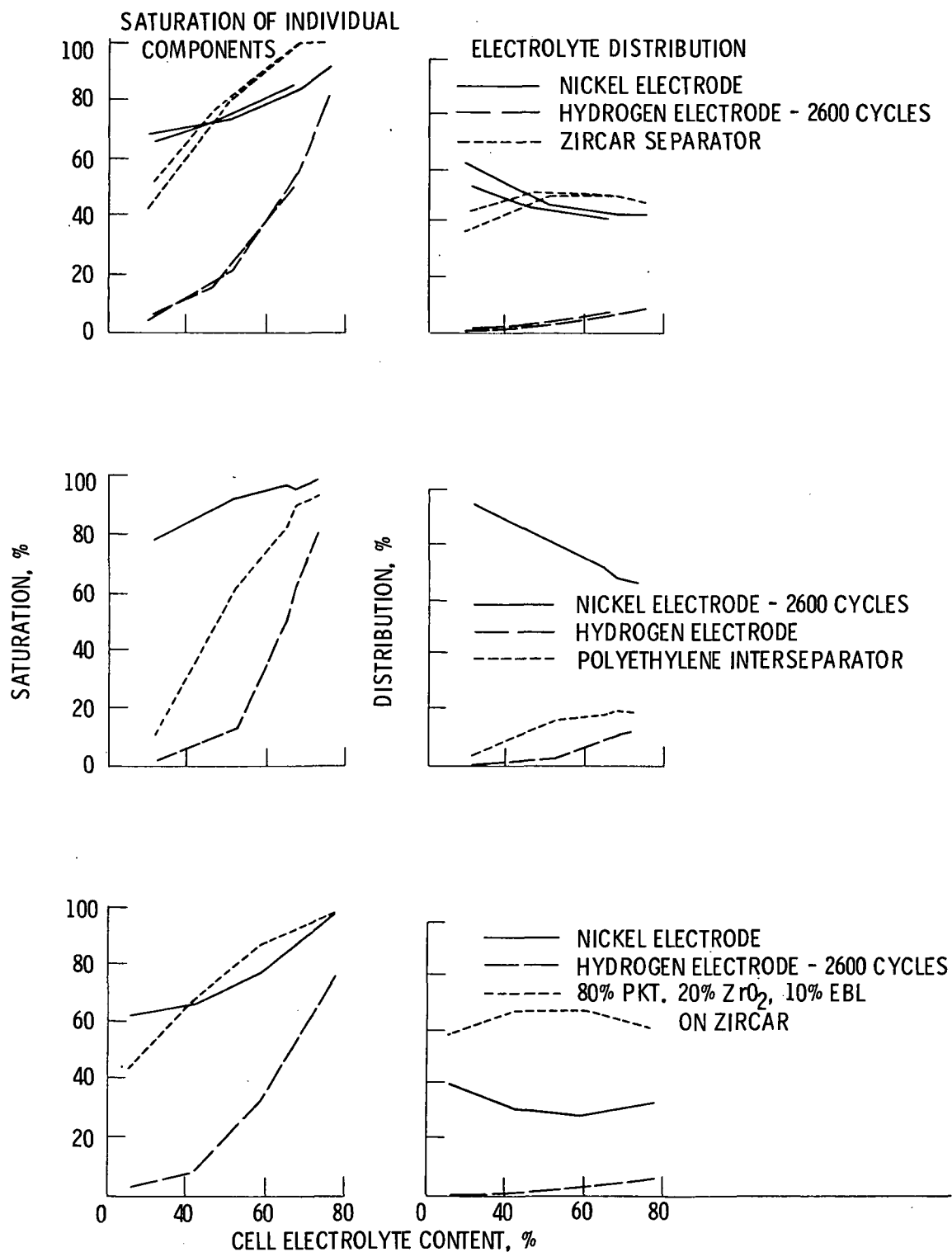Figure 14. - Electrolyte distribution curves for combination of Air Force electrodes and separators.

Figure 15. - Electrolyte distribution curves for combination of Air Force electrodes and separators.
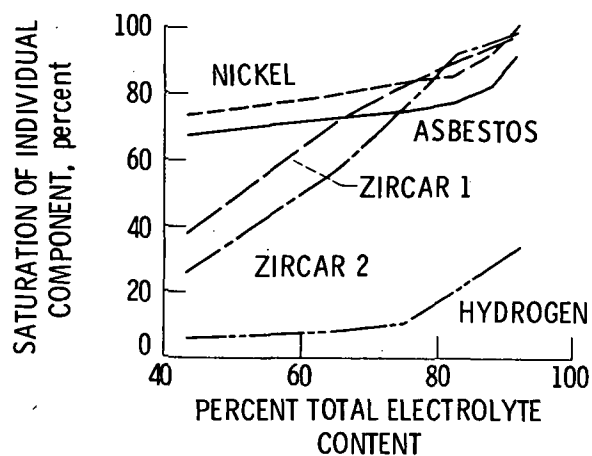
Figure 16. - Percent saturation of individual components for model system.
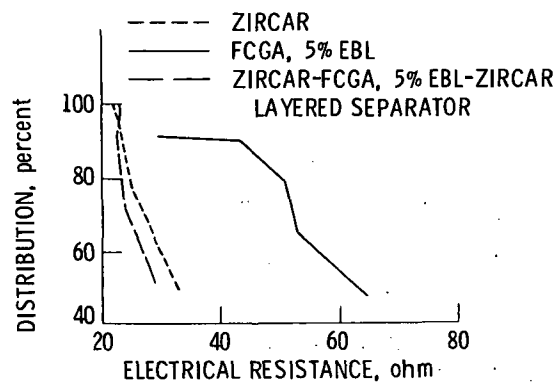
Figure 17. - Resistance measurement curves for combination of Air Force nickel, 2600 cycled Air Force hydrogen and separators.
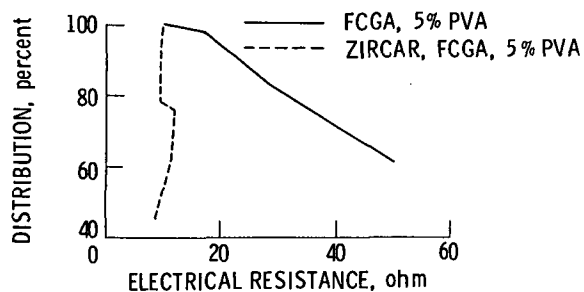
Figure 18. - Resistance measurement curves for combination of Air Force nickel, hydrogen from a silver/hydrogen cell and separators.

1. Report No. NASA TM-83073	2. Government Accession No.	3. Recipient's Catalog No.
4. Title and Subtitle ELECTROLYTE MANAGEMENT IN POROUS BATTERY COMPONENTS - STATIC MEASUREMENTS		5. Report Date
		6. Performing Organization Code 506-55-52
7. Author(s) Kathleen M. Abbey and Doris L. Britton		8. Performing Organization Report No. E-1545
		10. Work Unit No.
9. Performing Organization Name and Address National Aeronautics and Space Administration Lewis Research Center Cleveland, Ohio 44135		11. Contract or Grant No.
		13. Type of Report and Period Covered Technical Memorandum
12. Sponsoring Agency Name and Address National Aeronautics and Space Administration Washington, D. C. 20546		14. Sponsoring Agency Code

15. Supplementary Notes

Prepared for the Autumn Annual Meeting of the Electrochemical Society, Detroit, Michigan, October 17-22, 1982.

16. Abstract

The interaction between the porous hydrogen and nickel electrodes and microporous separator with respect to electrolyte management in nickel/hydrogen cells has been investigated. The distribution of electrolyte among the components has been measured and correlated with the pore size distributions, total void volume, and resistance of a variety of electrodes and separators. Calculations are used to show the effects of systematically varying these properties.

17. Key Words (Suggested by Author(s)) Electrolyte management Porous electrodes Batteries	18. Distribution Statement Unclassified - unlimited STAR Category 25

19. Security Classif. (of this report) Unclassified	20. Security Classif. (of this page) Unclassified	21. No. of Pages	22. Price*

National Aeronautics and
Space Administration

Washington, D.C.
20546

SPECIAL FOURTH CLASS MAIL
BOOK

NASA